Analytical and Bioanalytical Chemistry
https://doi.org/10.1007/s00216-022-04294-y

RESEARCH PAPER

Mass spectrometry–based metabolomic signatures of coral bleaching under thermal stress

Ji-Ying Pei[1] · Wen-Feng Yu[1] · Jing-Jing Zhang[1] · Ting-Hao Kuo[2] · Hsin-Hsiang Chung[2] · Jun-Jie Hu[1] · Cheng-Chih Hsu[2] · Ke-Fu Yu[1,3]

Received: 4 June 2022 / Revised: 19 July 2022 / Accepted: 17 August 2022

Abstract

Coral bleaching caused by climate change has resulted in large-scale coral reef decline worldwide. However, the knowledge of physiological response mechanisms of scleractinian corals under high-temperature stress is still challenging. Here, untargeted mass spectrometry–based metabolomics combining with Global Natural Product Social Molecular Networking (GNPS) was utilized to investigate the physiological response of the coral species *Pavona decussata* under thermal stress. A wide variety of metabolites (including lipids, fatty acids, amino acids, peptides, osmolytes) were identified as the potential biomarkers and subjected to metabolic pathway enrichment analysis. We discovered that, in the thermal-stressed *P. decussata* coral holobiont, (1) numerous metabolites in classes of lipids and amino acids significantly decreased, indicating an enhanced lipid hydrolysis and aminolysis that contributed to up-regulation in gluconeogenesis to meet energy demand for basic survival; (2) pantothenate and panthenol, two essential intermediates in tricarboxylic acid (TCA) cycle, were up-regulated, implying enhanced efficiency in energy production; (3) small peptides (e.g., Glu-Leu and Glu-Glu-Glu-Glu) and lyso-platelet-activating factor (lysoPAF) possibly implicated a strengthened coral immune response; (4) the down-regulation of betaine and trimethylamine N-oxide (TMAO), known as osmolyte compounds for maintaining holobiont homeostasis, might be the result of disruption of coral holobiont.

Keywords Metabolomics · Mass spectrometry · Bleaching · Thermal stress · Lipid metabolism

Introduction

Coral reefs, as one crucial marine ecosystem, possess high productivity and species diversity. They provide essential services, such as fisheries habitat, tourism, and coastal protection, to millions of people worldwide. In the past decades, coral reef ecosystems have faced an unprecedented threat imposed by global climate change [1, 2]. Global warming has caused extensive coral bleaching [3, 4], which can further lead to coral mortality and the destruction of the structure and function of the coral reef ecosystem [4, 5]. Coral bleaching is the result of dysfunction of the symbiotic relationship and expulsion of the symbiont from a coral host. With the occurrence of bleaching, the normal bi-directional exchange of metabolites between the coral host and Symbiodiniaceae is destroyed. However, the knowledge of the physiological response mechanisms of coral holobiont during high-temperature stress is limited.

Recent advances in the omics fields [6, 7] (genomics, transcriptomics, proteomics, and metabolomics) have provided new knowledge about the biological mechanisms implicated in coral response to thermal stress. Metabolomics focuses on the end products of cellular regulatory processes that link genotype, phenotype, and the environment, and it can amplify the small differences in gene variation or protein expression. Intracellular metabolite pools play crucial roles in cellular homeostasis, including antioxidation [8], signal transduction [9], and energy

✉ Ke-Fu Yu
kefuyu@scsio.ac.cn

[1] Coral Reef Research Center of China, Guangxi Laboratory On the Study of Coral Reefs in the South China Sea, School of Marine Sciences, Guangxi University, Nanning, Guangxi 530000, People's Republic of China

[2] Department of Chemistry, National Taiwan University, Taipei 10617, Taiwan

[3] Southern Marine Science and Engineering Guangdong Laboratory, Zhuhai, Guangdong 519080, People's Republic of China

Published online: 05 September 2022

generation [10] as well as the synthesis of complex secondary compounds through primary metabolites [11]. Confronting environmental stress, the metabolites might be adjusted to minimize the injury. For example, betaines, as compatible solutes, can stabilize membrane structure to protect photosynthesis of Symbiodiniaceae from high irradiance or unusual temperature stress [12, 13]. As a result, the study of metabolic networks in complex systems serves as a reliable tool for elaborating cellular response to environmental stress. However, few studies [14–20] have applied metabolomics to explore the underlying molecular mechanism of coral response to high-temperature stress. By the paired metabolome analysis of historically unbleaching and bleaching (but recovered) *Montipora capitata*, betaine lipids were found to be the strongest metabolite drivers for differentiating historical bleaching phenotype, providing a new tool for screening heat-resistant coral [18]. Microorganisms are vital components of coral holobiont, and the virulence of some pathogens, such as *Vibrio coralliilyticus*, boosted with rising temperature. Nuclear magnetic resonance (NMR)–based metabolomics has revealed that the adjustment of the metabolic pathways of the pathogen played a role in the enhanced pathogenicity when the environmental temperature was elevated [21].

Recently, mass spectrometry–based metabolomics approaches have enabled the exploration of the chemotype of various complex biological systems [14]. Here, an untargeted mass spectrometry–based metabolomics approach combined with Global Natural Product Social Molecular Networking (GNPS) [22, 23] was used to explore the molecular regulatory mechanisms of reef-building corals in response to high-temperature stress. Considering that the dominant species of corals have shifted to bleaching-tolerant coral worldwide [24–26], and high latitude may serve as a potential refuge for corals under global warming [26], in this study, the bleaching-tolerant coral *Pavona decussata* collected from Weizhou island located in a relatively high latitude area in the northwestern South China Sea (SCS) was used as the model coral to investigate the molecular adaptive mechanism of stress-hardened corals under future global warming. After cultivating the heat-stressed *P. decussata* in an artificial aquarium, a liquid chromatography–mass spectrometry (LC–MS) was utilized to characterize their metabolites associating with physiological changes. Then, GNPS was used to deduce unknown metabolites based on annotated compounds. The possible biochemical mechanisms involved in the potential biomarkers of lipid, peptide, and small-molecule metabolites were demonstrated. This study provides an insight into the molecular mechanism underlying the response of *P. decussata* to thermal stress, laying the foundation for conservation and restoration of the coral reef ecosystem in the content of global climate warming.

Materials and method

Collection and cultivation of coral nubbins

The coral *P. decussata* with a size of four square decimeters was sampled from Weizhou island (N21°07′, E109°14′, Guangxi, China) on 20 May 2019 using a hammer and chisel at a depth of 9–10 m, and transported to the aquaria in Guangxi University in 3 h. The coral was identified based on its ecological and morphological characteristics. After acclimatization to the aquarium for 30 days, a coral colony was fragmented into 10 pieces and glued to labelled aragonite plugs with epoxy adhesive. The 10 glued nubbins were then randomly distributed between two aquaria, and continued to acclimate to the ex situ conditions for 30 days. Continuous flow-through seawater (average flow rate of 3 L/min) was prepared with synthetic sea salt. The water movement in each aquarium was provided by small submersible pumps (CP-55, Zhongshan Jiebao Electronic Appliance Co., Ltd., Zhongshan, China). Each tank was equipped with a temperature-controlled system (Water Cooler, Hailea, Model: HS-66A, temperature detector: Caperplus C1). The light was set for a 12-h light–dark cycle using T5HO lights (Zhongshan Songbao Electronic Appliance Co., Ltd., Zhongshan, China).

The temperature programming is shown in Fig. 1a. After acclimation, we subjected the coral nubbins to heat stress with programmed temperature elevation or a controlled temperature at 26 °C. The heating program was set as follows: increase by one degree every 12 h, and acclimatize to 60 h when the temperature was elevated by 3 °C. This process was circulated till the temperature reached 35 °C, and then the temperature was maintained at 35 °C for 72 h before sampling.

Daily measurements of maximum and actual quantum yield of photosystem II (PS II) (Fv/Fm) were taken using pulse amplitude modulation (PAM) fluorometry (Diving-PAM, Walz, Effeltrich, Germany). Maximum quantum yields were taken after stop illuminating for 30 min for coral adaptation to darkness, while the real-time quantum yield of PS II was measured with the light on. The distance between PAM fluorometry and the coral surface was set as 3 mm. Triplicate measurements were taken from each coral fragment. The PAM parameters were set as follows: measuring light, 4; saturation intensity, 4; saturation width, 0.6 s; gain, 1; and damping, 2 with the use of the measuring light burst function.

Fragment processing

The coral fragments were placed into liquid nitrogen instantly when taken from the aquarium, and then stored

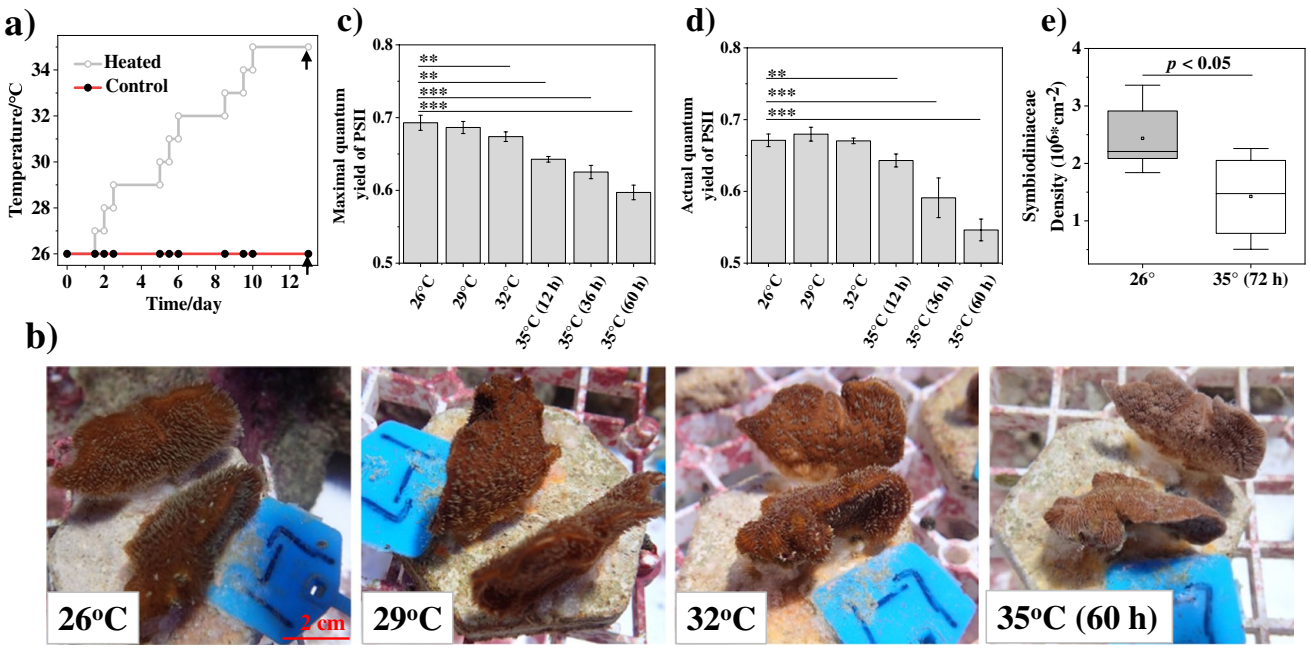

Fig. 1 **a** The programmed temperature in the coral aquarium. Arrows represent the sampling time. **b** Effects of temperature on coral morphology. **c** Maximum and **d** actual quantum yield of PSII of corals. $^{*}p<0.05$, $^{**}p<0.01$, $^{***}p<0.001$. **e** Comparison of Symbiodiniaceae density between corals at 26 °C and 35 °C (72 h).

in a − 80 ℃ refrigerator before subsequent treatment. Coral tissue from a fragment was removed by Waterpik with 50 mL chilled ultrapure milli-Q water. The water was circularly used to flush the coral until the skeleton's tissues were completely peeled off. One mL tissue suspension was used for Symbiodiniaceae cell counts, and the other 49 mL was lyophilized to dry powder for metabolite extraction.

Measurement of Symbiodiniaceae cell density

Symbiodiniaceae cell densities were quantified from 1 mL aliquots of tissue suspensions using improved Neubauer hemocytometer counts (Boeco, Germany) with six replicate measurements. Cell density was normalized to coral fragment surface area, measured with the tinfoil-wrapping method [27, 28].

Metabolite extraction from coral nubbins

Metabolites were extracted from dried coral tissue powder using ultrasonic extraction and vortexing (Figure S1). Briefly, 0.5 mL of ice-cold methanol/water (v/v, 7:3) containing an internal standard (caffeine-D9, 2 µg/mL) was added to a pre-weighed coral tissue powder (10 mg) in a 2 mL sample tube. After alternating ultrasonication and vortexing for 3 min, samples were centrifuged at 12,000 × *g* for 3 min at 4 °C. The supernatant was collected and temporarily stored on dry ice. This procedure was performed thrice to ensure the complete extraction of the metabolites. The combined extract was filtered through a 0.22-µm nylon syringe filter and stored at − 80 °C until LC–MS/MS analysis.

Mass spectrometry data collection and pre-processing

Coral metabolite extracts were analyzed on a Thermo™ Q-Exactive™ mass spectrometer coupled to a Dionex UltiMate 3000 UHPLC system. The mobile phase A and B were H_2O with 0.1% formic acid and methanol with 0.1% formic acid, respectively. The chromatographic separation was performed using ACQUITY CSH C_{18} column (2.1 × 100 mm; 1.7 µm; Waters, MA, USA) with a flow rate of 200 µL/min at 30 °C using the following gradients: 0–3 min, 5% B; 3–20 min, 5–95% B. Ninety-five percent B was held for 5 min followed by a switch to 5% B in 1 min, and then maintained for 4 min to reach system stability before next injection. The injection volume of each sample was 2 µL. Data was collected in positive electrospray ionization mode with the data-dependent acquisition (DDA). A DDA method was performed by scanning a full MS from *m/z* 100 to 1000 and collecting MS/MS spectra of the top 10 most intense compounds.

Raw files (.raw) were converted to.mzXML format, and analyzed using open-source MZmine software (v2.51) to extract chromatographic features. Feature extraction for full MS and MS/MS spectra was performed with an exact

mass detector with a signal threshold of 70,000 and 10,000 respectively. The chromatogram building was achieved using a minimum height of 70,000, and *m/z* tolerance of 0.001 (or 5 parts per million (ppm)). Chromatograms were deconvoluted by the local minimum algorithm with a peak duration range of 0.07 to 1.20 min, and a minimum absolute height of 70,000. Isotopic peaks were grouped with an *m/z* tolerance of 0.003 Da (or 12 ppm), and a retention time tolerance of 0.05 min. Detected peaks were aligned through Join Aligner Module with *m/z* tolerance of 0.02 Da, and retention time tolerance of 0.02 min. The resulting peak list was gap filled with intensity tolerance of 5%, *m/z* tolerance of 0.001 Da (or 5 ppm), and retention time tolerance of 0.15 min. The signal intensities of all metabolites were normalized by the signal intensity of caffeine-D9. A complete description of instrument and software parameters is provided in Table S1.

Molecular network analysis

A.mgf-formatted file and a feature quantification table exported from MZmine software were uploaded to the GNPS website for running feature-based molecular networking (FBMN) workflow. FBMN was performed with a parent and fragment mass ion tolerance of 0.02 Da, a cosine score of 0.7, a minimum matched peaks of 2, library search minimum matched peaks of 2, a library search score threshold of 0.7, and a minimum peak intensity of 20,000. Feature-based molecular networking job is available at: https://gnps.ucsd.edu/ProteoSAFe/status.jsp?task=787a1543ace64f2586e19c16ec305655.

The FBMN output files were visualized using Cytoscape (v3.8.0). In total, 147 compounds were annotated by GNPS library search. With the annotated compounds as "seeds," we could infer adjacent unknown nodes according to the MS/MS spectra. To seek more "seeds" in the molecular network, metabolite identification was also performed by Compound Discoverer 3.2 software (Thermo Fisher Scientific, USA) with detailed parameters provided in Table S2. This resulted in the identification of additional 59 compounds with the standard of mzCloud Best Match > 80. For annotated metabolites with variable importance in the projection (VIP) > 1, the MS/MS spectra were manually inspected to avoid false matches.

Statistical analysis

The processed data were introduced to SIMCA-P (v14.1, Umetrics, Umea, Sweden) for principal component analysis (PCA) and partial least square discriminant analysis (OPLS-DA). All data were unit variance (UV) (for PCA) or Pareto (Par) (for OPLS-DA)-scaled before multivariate statistical analysis. The predictivity of sevenfold cross-validated OPLS models was validated through 200 random permutations of the class membership variable. The significance of the goodness-of-fit and goodness-of-prediction were assessed by R^2(cum) (explained variance) and Q^2(cum) (predicted variance) parameters, respectively. When R^2Y(cum) and Q^2(cum) are close to 1, the model is considered excellent; when $Q^2 \geq 0.5$, the model is considered reliable. Variable Importance in the Projection (VIP) > 1.0 is supposed to contribute significantly to the separation. A two-tailed unpaired Student's *t*-test was used for significance testing, and *P* values less than 0.05 were considered significant.

The unsaturation index (UI) for each lipid class was calculated using the following formula:

$$\mathrm{UI}_x = \left[\sum y\left(\%\mathrm{lipid}_y \times \text{total number of double bonds lipid}_y\right)\right]/100$$

where *y* is every molecular lipid species belonging to the lipid class *x*.

Pathway enrichment analysis

The online metabolic data analysis platform Metaboanalyst 5.0 (https://www.metaboanalyst.ca/) [29] was used for pathway enrichment analysis based on the potential biomarkers, and the enrichment analysis was conducted based on the KEGG database (https://www.genome.jp/kegg/pathway.html).

Data quality control

A quality control (QC) sample was prepared by mixing an equal quantity of each coral tissue dry powder, and extracted by the same method as samples. The pooled QC sample was injected five times in the beginning to ensure system equilibrium and injected every five samples during LC–MS analysis to monitor system stability. The coefficient of variance (CV) of the metabolites in the QC samples was on average 7%. A blank solution, which matched the composition of the extraction solvent, was injected every three samples (before the QC detection) to assess background signals and ensure that there was no carryover during analysis. All known metabolites in the mixture were detected within 5 ppm mass accuracy.

Results

Changes in physiological phenotypes, PSII quantum yield, and Symbiodiniaceae density of P. decussata

Our lab-built coral aquarium served as a temperature-tunable apparatus to examine changes in *P. decussata* physiological

phenotypes and determine their corresponding quantum yield and Symbiodiniaceae density. By applying a programmed heating process to the aquarium (Fig. 1a), we successfully induced coral bleaching as recorded in Fig. 1b. In the beginning, when the environment was heated from 26 to 29 °C, most of the coral tentacles began to contract whereas only a small portion of the tentacles underwent extension. Then, the proportion of the extended tentacles decreased as the temperature further rose to 32 °C. Finally, the tentacles fully contracted in company with coral whitening when the temperature reached 35 °C. During the programmed heating process, the maximum and actual quantum yield of PSII was measured periodically at 26 °C, 29 °C, 32 °C, and 35 °C. The maximum quantum yield of PSII declined from 0.69 to 0.60 when the temperature was elevated from 26 to 35 °C (60 h) (Fig. 1c). The actual quantum yield of PSII showed random fluctuation during 26–29 °C, and then gradually decreased when the temperature reached 35 °C (Fig. 1d). Regarding Symbiodiniaceae density, we discovered that the thermal stress resulted in a significant decrease from $2.44*10^6$ cell cm^{-2} (26 °C) to $1.42*10^6$ cell cm^{-2} (35 °C, 72 h) ($p < 0.05$) (Fig. 2e).

Metabolomic profiling of heat-stressed and healthy coral

To reveal metabolic markers indicative of coral bleaching, the metabolite extracts of heat-stressed and healthy corals were subject to untargeted metabolomic investigation and multivariate data analyses. As a result, a total of 1636 unique metabolite features were extracted from the untargeted metabolomics dataset, representing the chemical diversity of the coral system. Multivariate data analyses were employed to better visualize the subtle difference in the metabolome between heat-stressed and healthy corals. PCA, an unsupervised method, was employed to reduce the dimensionality of the data while retaining most of the variation (Fig. 2a), showing that the corals exposed to high temperature (treatment group) were visibly separated from those exposed to 26 °C (control group) (R^2X(cum) = 0.550, Q^2(cum) = 0.400). Additionally, OPLS-DA, a supervised method, was further applied to build another classification model. The results indicated that the metabolic profile of the treatment group deviated from that of the control group (R^2Y(cum) = 0.988, Q^2(cum) = 0.922) (Fig. 2b). The 7-round cross-validation and 200 random permutation test showed good predictability without overfitting in the OPLS-DA model (Figure S2). S-plots were constructed to identify metabolites that distinguished the bleaching corals from controls (Fig. 2c). There were 215 metabolite features that were initially screened out with the criterion of VIP > 1. These features were further screened by Student's *t*-test, giving 170 significant metabolites ($p < 0.05$) that were potential metabolic biomarkers to coral bleaching.

Metabolite identification with GNPS

In the coral metabolome, the identification of 215 significant metabolites (VIP > 1) remained unknown. To deduce their structures, the metabolomic dataset was further processed by GNPS, creating a molecular network that showed structural similarity between metabolites. In the molecular network, structural analogues are connected to form molecular clusters, and this feature strategically facilitates the annotation of unknown metabolites by their connected knowns. Here, we showed that the *P. decussata* molecular network encompassed dozens of molecular clusters (number of nodes > 2). Meanwhile, 867 metabolites were down-regulated and 769 metabolites were up-regulated (Figure S3). In the metabolome, up to 206 metabolites were putatively annotated by the GNPS spectral libraries and databases in Compound Discoverer, and served as "seeds" for identifying their neighboring unknowns. In the OPLS-DA

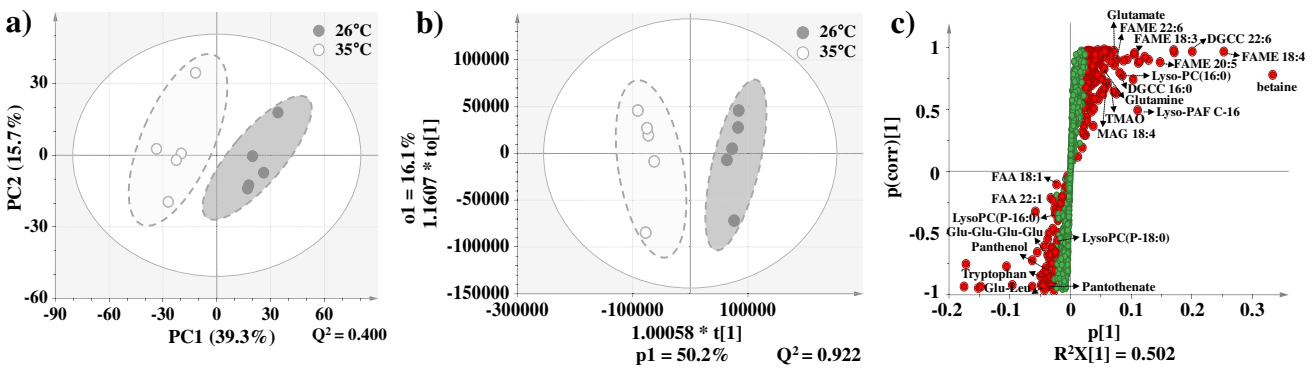

Fig. 2 Multivariate analysis of LC–MS data obtained from the bleaching corals (35 °C) and controls (26 °C). **a** Score plots of PCA and **b** OPLS-DA, **c** S-plot of the OPLS-DA model

model, betaine was the strongest metabolite driver which differentiated heat-bleaching corals from healthy ones. The second strongest metabolite driver was an unknown compound of *m/z* 562.3728 (number of VIP (N_{VIP}) = 3) connected to a molecular family where the metabolite of *m/z* 490.3735 was annotated as a betaine lipid: diacylglyceryl-carboxyhydroxymethylcholine (DGCC) 16:0 (Fig. 3a). By aligning the MS/MS spectra, we discovered that the unknown metabolite *m/z* 562.3728 and DGCC 16:0 shared common fragment ions indicative of the loss of a betaine head group (e.g., *m/z* 104.1073 and *m/z* 132.1020). By inferring the desaturation degree and length of the fatty acyl chain from exact mass, this unknown metabolite was identified as DGCC 22:6. Similarly, the other biomarkers (VIP > 1, $p < 0.05$) in this molecular family were identified as betaine lipids (Figure S4), and they all showed lower abundance in heat-stressed corals (Table S3). The third strongest metabolite driver of differentiating heat-bleaching and healthy corals was an unknown metabolite of *m/z* 291.2318, connected to a large molecular family in which 44% metabolites (29 out of 66) were potential biomarkers (Figure S5). In the 29 potential biomarkers, 16 of them were putatively annotated by the GNPS libraries as various classes of lipids (fatty acid (FA), fatty acid amide (FAA), fatty acid methyl ester (FAME), and monoacylglycerol (MAG)). By investigating MS/MS spectral similarity between the unknown metabolites in this molecular family, we identified the third strongest metabolite driver *m/z* 291.2318 as FAME 18:4 (Figure S6) and the majority of the other unknown metabolites as lipids of various

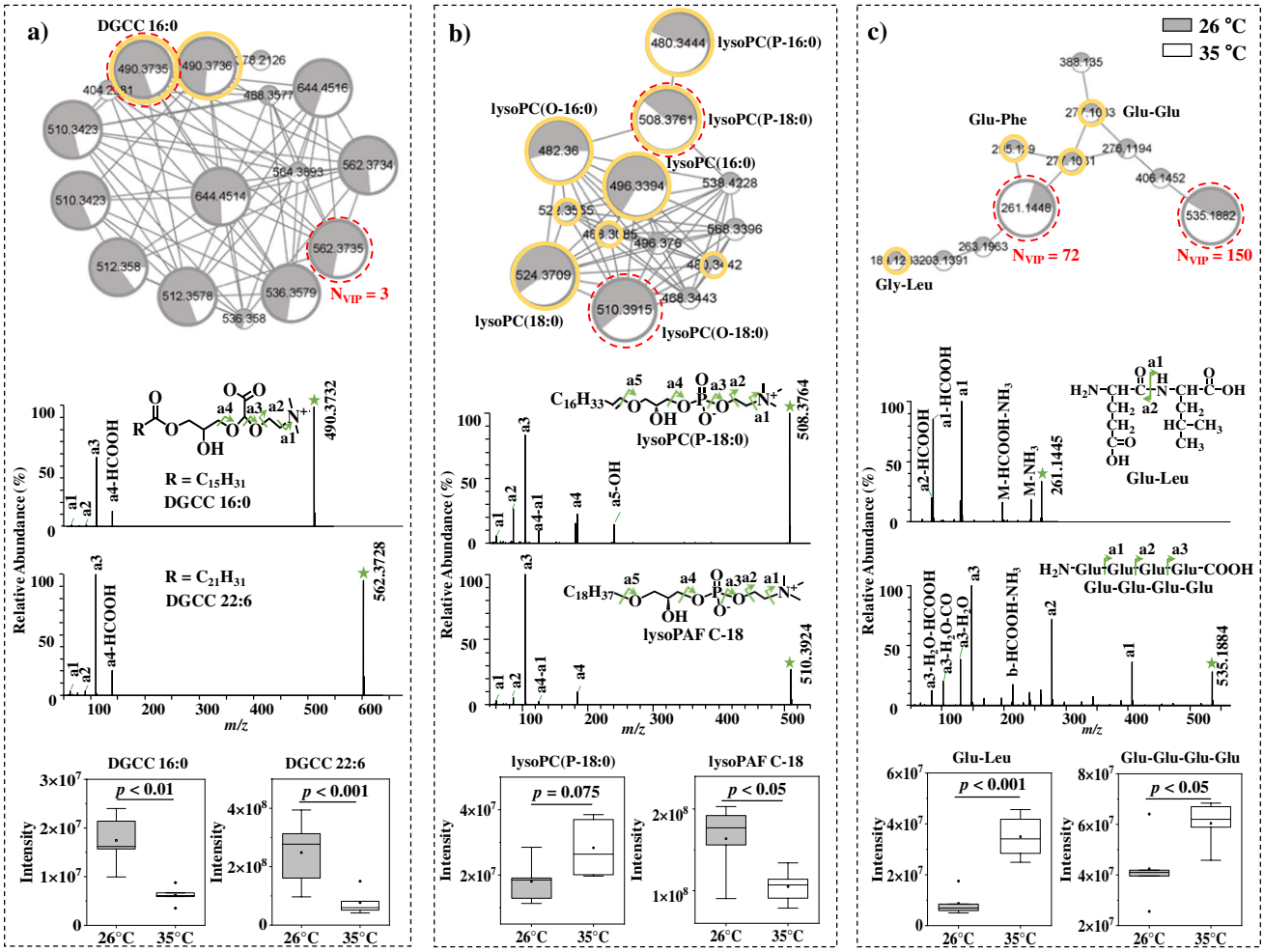

Fig. 3 Molecular network, MS/MS spectra, and boxplots of the (**a**) betaine lipid molecular family, (**b**) PC family, (**c**) peptide family. Each node in the network represents a unique metabolite and is labelled by the parent mass. The nodes with bigger circles represent potential biomarkers with VIP > 1. The gray-white pie graph in each node shows the abundance of each metabolite in either bleached corals (white, 35 °C) or controls (gray, 26 °C). The nodes labelled with yellow circles represent compounds annotated by the databases (GNPS or Compound Discoverer). The MS/MS spectra and boxplots showing the variation of the signal intensities of the compounds labelled with red dotted circles between bleached corals and controls are displayed. MS/MS spectra are shown along with putative chemical structures with undetermined unsaturation positions. Boxplots are median with quartiles and whiskers extending 1.5 IQR beyond quartiles

classes (FA, FAA, FAME, MAG, monogalactosylmonoacylglycerol (MGMG), and digalactosylmonoacylglycerol (DGMG)) (Figure S6–10). Most of these lipids were down-regulated in heat-stressed corals (Table S3). Another important molecular family containing signatures of phosphorylcholine head group in its MS/MS pattern (characteristic fragment ions, *m/z* 86.0968, 104.1072, 184.0733) were identified as phosphatidylcholine (PC), plasmanylcholine (PC(O)), and plasmenylcholine (PC(P)) (Fig. 3b and Figure S11). While lysoPC(P-16:0) (*m/z* 480.3454, $N_{VIP} = 83$) and lysoPC(P-18:0) (*m/z* 508.3767, $N_{VIP} = 203$) were up-regulated in heat-stressed corals, on the contrary, lysoPC(16:0) (*m/z* 496.3340, $N_{VIP} = 23$), lysoPC(18:0) (*m/z* 524.3711, $N_{VIP} = 59$), lysoPC(O-16:0) (*m/z* 482.3611, $N_{VIP} = 8$) (namely lyso-platelet-activating factor (lysoPAF) C-16), and lysoPC(O-18:0) (*m/z* 510.3924, $N_{VIP} = 39$) (namely lysoPAF C-18) were down-regulated (Table S3).

Furthermore, two important potential diagnostic biomarkers with *m/z* 261.1445 ($N_{VIP} = 72$), and *m/z* 535.1884 ($N_{VIP} = 150$) were identified as glutamate-leucine (Glu-Leu) and glutamate-glutamate-glutamate-glutamate (Glu-Glu-Glu-Glu) with characteristic fragment ions representative to loss of Glu monomer (Fig. 3c). Their abundances were up-regulated in heat-stressed corals compared to healthy corals, especially Glu-Leu whose abundance was enhanced four times (Table S4).

Other potential biomarkers, such as glutamine, glutamate, aspartate, tryptophan, pantothenate, panthenol, betaine, trimethylamine N-oxide (TMAO), and inosine, were also identified by library search and manual interpretation with the assistance of molecular networking (Figures S12–S13). Among these biomarkers, tryptophan, panthenol, and pantothenate were up-regulated, while the others were down-regulated when corals faced temperature stress (Table S4). In clustering analysis of these 15 potential small-molecule biomarkers, the bleaching corals were separated from the healthy ones (Figure S14).

For the 215 metabolites with VIP > 1, lipid, small molecules, and unknown metabolites accounted for 25.6%, 14.9%, and 58.1%, respectively (Figure S15). Structural lipids (betaine lipid, PC, DGCC, MGMG, DGMG) and storage lipids (FA, FAA, MAG) accounted for 55.7% and 44.3% of the total lipid biomarkers respectively. To compare the change of the physicochemical property of the holobiont membrane, the UI based on the potential biomarkers of structural lipids was calculated. The results showed a lower UI in heat-stressed corals as compared to controls (Figure S16).

Metabolic pathway analysis

To characterize how coral metabolome changed in response to heat stress, metabolic pathway enrichment analysis was performed by subjecting the above-mentioned potential biomarkers (VIP > 1, $p < 0.05$) to MetaboAnalyst software. To obtain more robust results, lipids were excluded because their detailed structures (e.g., double bond position) were ambiguous. Additionally, Glu-Leu and Glu-Glu-Glu-Glu were excluded due to their absence in the KEGG database. Finally, 12 biomarkers were imported to MetaboAnalyst software for pathway enrichment analysis (Table S5), showing that 18 metabolic pathways (glutamine and glutamate metabolism, arginine biosynthesis, nitrogen metabolism, alanine, aspartate and glutamate metabolism, histidine metabolism, pantothenate, and acetyl coenzyme A (CoA) biosynthesis to name

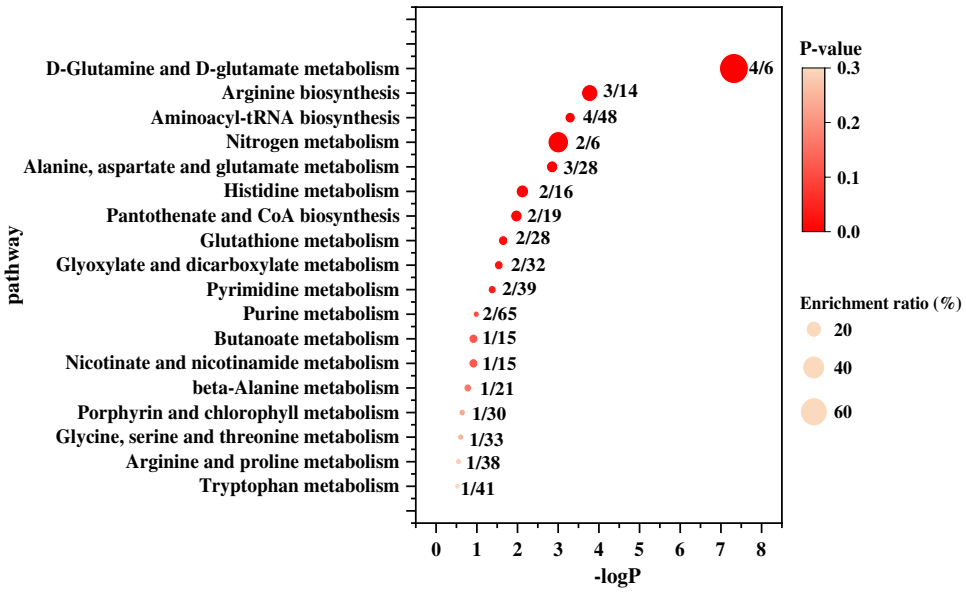

Fig. 4 Metabolic pathway enrichment analysis of corals exposed to thermal stress. The numbers before and after the oblique line represent observed potential biomarkers and total metabolites in the metabolic pathway respectively

a few) were perturbed when the corals responded to high-temperature stress (Fig. 4). These metabolic pathways highlighted the metabolism of amino acid and cofactor. For example, glutamate, glutamine, and aspartate were enriched in amino acid metabolism, while pantothenate and panthenol were enriched in CoA metabolism.

The disrupted CoA metabolic pathway is depicted in Fig. 5. Aspartate-α-decarboxylase catalyzes the decarboxylation of aspartate to generate alanine, and alanine reacts with pantoate to produce pantothenate. Following a series of reactions (phosphorylation, condensation reaction with cysteine, decarboxylation, and AMP transfer), pantothenate is converted to CoA that subsequently participates in the TCA cycle. Pantothenate is also the metabolic product of panthenol in this pathway.

The disrupted amino acid metabolic pathway is shown in Figure S17. Glutamine and glutamate could be mutually converted via the glutamine synthetase/glutamine:2-oxoglutarate aminotransferase cycle in the pathways of glutamine and glutamate metabolism, nitrogen metabolism, and alanine, aspartate, glutamate metabolism, histidine metabolism, and arginine biosynthesis. In that cycle, ammonium is added to glutamate (Glu) to produce glutamine (Gln); Gln is then converted back to Glu with either glutamate synthase or glutaminase.

Discussion

The data presented herein illustrate biochemical and metabolic abnormalities of corals that are exposed to thermal stress. In the heat-stressed corals, the declined Symbiodiniaceae density and maximum and actual photochemical efficiency of PSII indicated photoinhibition, symbiosis breakdown, and coral bleaching. Generally, corals rely on tentacle motion to support their respiration, photosynthesis, prey capture, heat exchange, and reproduction [30]. To reduce exposure to high-temperature stress, the tentacle of coral polyps contracted. Besides the physiological response mentioned above, the metabolic pathways of corals were adjusted in response to high-temperature stress.

Dysfunction of various lipid metabolic pathways by high-temperature stress

The total coral lipids can be generally viewed as the combination of three types of lipids: storage lipids (such as FAME and MAG), structural lipids (such as DGCC and lysoPC), and glycolipids (such as MGMG and DGMG). In principle, storage lipids determine the energy balance of corals; structural lipids serve as important components of the cell membrane; glycolipids are the crucial lipid of thylakoid membranes of Symbiodiniaceae [31]. Traditionally, the FA 18:4, which mainly esterifies coral glycolipids, is considered characteristic of Symbiodiniaceae. However, a recent genomic study of desaturate enzymes in corals has challenged the long-held assumption that corals cannot synthesize polyunsaturated FA 18:4 [32]. Even though, it has been reported that zooxanthellate coral species have a higher content of FA 18:4 than azooxanthellate coral species [33], suggesting that the content of FA 18:4 were expected to correlate with the Symbiodiniaceae density in coral tissues. Based on these findings, the decline of MGMG, DGMG, and FA 18:4 in the heat-stressed coral holobiont in the present study could indicate the loss of Symbiodiniaceae from the coral host.

Under stress, corals allocate energy preferentially towards basic survival. After available ATP and stored glucose being

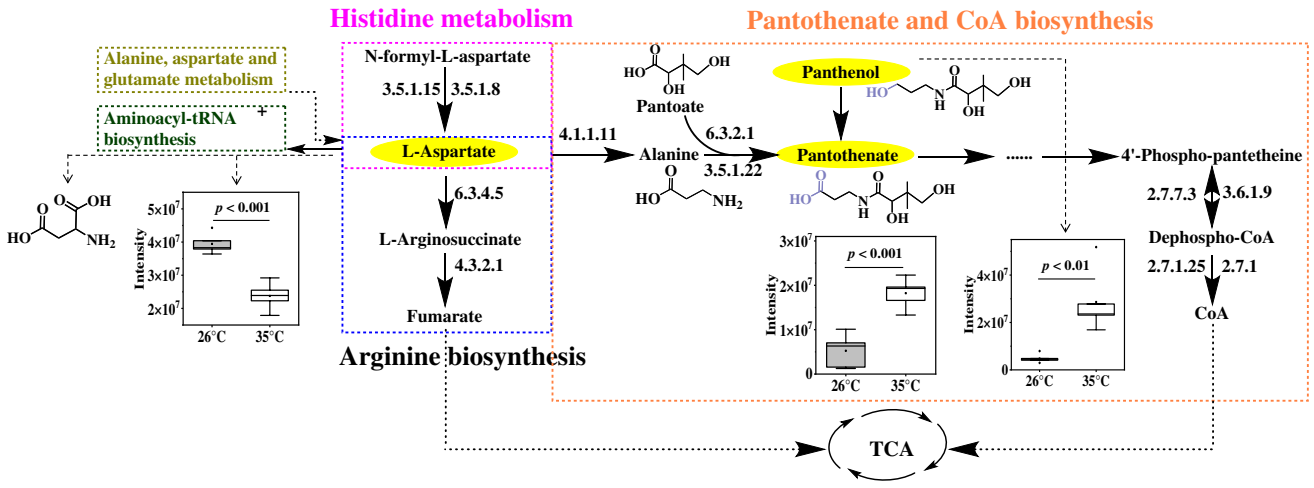

Fig. 5 The perturbed metabolic pathways (histidine metabolism, arginine biosynthesis, pantothenate, and CoA biosynthesis) involved the three potential biomarkers (aspartate, pantothenol, and pantothenate) when corals responded to thermal stress. Boxplots show the abundance change of metabolites between bleached corals (white, 35 °C) and controls (gray, 26 °C)

consumed, hydrolysis of storage lipid would be activated to compensate for energetic demands, and elevated temperature accelerated the rate of lipid depletion, which suggested that the basic metabolism became more energetically costly [34]. However, we observed that the biosynthesis of storage lipid by algal was dampened due to photosynthesis inhibition under heat stress, possibly resulting in the decrease of storage lipids as similarly observed in previous studies [35, 36]. On the other hand, Symbiodiniaceae resides in the endoderm of coral animals and is covered by a host-derived membrane [37]. Expulsion of Symbiodiniaceae from coral cells could damage the structure of coral cell membrane, resulting in the loss of structural polar lipids, such as DGCC, PC, and CerP. Additionally, the biosynthesis of DGCC varied with Symbiodiniaceae species; for example, thermosensitive *Cladocopium* C3 has a higher content of DGCC than thermotolerant *Durusdinium trenchii* [38]. The loss of thermosensitive Symbiodiniaceae under thermal stress conditions might result in the decline of DGCC [39, 40].

PAF and lysoPAF are coral host-derived central inflammatory modulators that participate in the coral defense against environmental stress [41], and are believed to play an essential role in coral self/non-self-recognition and immune response. Under stress conditions, the inactivated form, lysoPAF, could be converted to the activated form, PAF, with the catalysis of lysoPAF acetyltransferase [15]. For example, when corals were damaged during competitive interactions with other species [15, 41] or exposed to ultraviolet light irradiation [41], the expression of the gene encoding lysoPAF acetyltransferase was strengthened, accompanying the increase of PAF. The corals that survived from historical bleaching also possessed higher amounts of PAF than those from historical unbleaching [18]. Therefore, when *P. decussata* were exposed to thermal stress, the down-regulation of lysoPAF C-16 and lysoPAF C-18 implicated the participation of coral host immune modulation [42].

In the present study, the degree of saturation of the potential biomarkers of structural lipids in heat-stressed *P. decussata* was higher. This result can be considered as a response of coral holobiont to prevent leakage of biological membranes at high temperature [38, 43], because lipid saturation affects the biophysical properties of the cell membrane, including thylakoid membrane melting point [44]. The up-regulation of lysoPC (P-16:0) and lysoPC (P-18:0) in heat-stressed *P. decussata* might result from the deficiency of the synthesis of polyunsaturated lysoPC [45].

Accumulation of peptides to resist high-temperature-induced oxidative stress

Peptides possess various biological functions, including antioxidant, signal transduction, and regulator [46]. For example, proline-arginine from salmon showed antioxidative activity against hydroxyl and superoxide anion radicals [47]; pyroGlu-Leu had the functions of hepatoprotection [48] and anti-inflammation [49]. More pieces of evidence have shown that bioactive peptides could decrease oxidative stress biomarkers (e.g., lipid peroxidation, intracellular ROS levels, apoptosis), increase activities of diverse antioxidant enzymes, and modulate levels of antioxidant molecules [47]. In our study, the accumulation of Glu-Leu and Glu-Glu-Glu-Glu in thermal-stressed *P. decussata* might be a response of the coral host to oxygen stress [19]. These peptides might be derived from proteolysis or insufficient peptide clearance [50].

Cooperation of various metabolites to maintain homeostasis of P. decussata holobiont

Thermal stress necessitates an increase in energy consumption and reallocates metabolic energy for maintaining cellular homeostasis. Tricarboxylic acid cycle (TCA) cycle, in which acetyl CoA catalyzes essential intermediary metabolism, is the primary source of energy production. In our results, the increased level of pantothenate and panthenol in heat-stressed corals might counteract the inefficiency of energy production, making energy production more costly. The accumulation of pantothenate in the TCA cycle could possibly suppress aspartate synthesis, resulting in the decreased content of aspartate.

Amino acids play critical roles in biosynthesis, growth, respiration via gluconeogenesis, and nitrogen recycling in alga-invertebrate symbiosis [51]. The decrease of various amino acids indicated dampened metabolism, which could be possibly attributed to three reasons: (1) photoinhibition resulted in the decline of nitrogen assimilation activity, reflected by the declined abundances of Glu and Gln, two sensitive indicators of nitrogen assimilation in coral symbiosis [52]. (2) The low efficiency of energy production under thermal stress could allocate energy preferentially to basic survival, resulting in the reduced activity of amino acid biosynthesis (a process consuming cellular energy). (3) The increased energy cost for maintaining homeostasis under elevated temperature could facilitate energy generation from an alternate pathway, such as amino acid metabolism via gluconeogenesis [14, 17].

TMAO and betaine are organic osmolytes that can assist stabilization of cellular molecular structure against thermal stress. For example, TMAO can increase protein thermal stability at an increased temperature [53] while acting as a cryoprotectant at a decreased temperature [54]. It has been reported that the production of TMAO from carnitine in humans shows inter-personal difference because TMAO metabolism depends on the gut microbiome whose

metabolic functions are heterogeneous between individuals [55]. In our study, the observed down-regulation of TMAO metabolism in heat-stressed corals could result from the change in microbial community because thermal stress could reassemble the community structure [56]. Last but not least, betaine (an osmolyte commonly found in plants, mammals, and bacteria) can assist cells to re-establish turgor pressure under increased osmolality conditions [21] and protect plants and algae against photosynthesis damage under high irradiance or unusual temperature stress [13]. Taken together, we speculated that the destruction of microbial and algae communities in coral holobiont by thermal stress could lead to the disorder of TMAO and betaine metabolism and thus destabilize cellular structures, which could consequently trigger coral bleaching.

Conclusion

In the present study, an untargeted mass spectrometry–based metabolomics method was applied to investigate how *P. decussata* coral metabolome is shaped by high-temperature-induced coral bleaching. By comparing the metabolic profiles between healthy corals and bleached corals, we detected a total of 60 metabolites (e.g., lipids, fatty acids, peptides, and some small-molecule metabolites) as potential biomarkers for coral bleaching. The regulation of these diverse coral metabolites and their associated metabolic pathways (lipid metabolism, peptide metabolism, amino acid metabolism, and other small-molecule metabolism) in response to heat treatment were characterized. Based on these results, we proposed the biochemical adaption of coral holobiont undergoing heat-induced bleaching process, as summarized in Fig. 6. Under heat stress, corals could activate the metabolic pathways of gluconeogenesis (such as lipid hydrolysis or aminolysis) to meet the energetic demands for basic survival, thus showing a corresponding decrease in a wide variety of storage lipids, fatty acids, and amino acids. The synthesis of two intermediates in the TCA cycle, pantothenate and panthenol, was strengthened to fortify the efficiency of energy production. Besides, the corals activated immune response and accumulated antioxidative peptides to defend corals against oxidative stress. Heat stress also suppressed the photosynthesis of Symbiodiniaceae dinoflagellate and affected nitrogen assimilation and amino acid levels. Additionally, small-molecule osmolytes that synergistically maintain holobiont homeostasis were declined upon coral bleaching; thereafter when the homeostasis was destabilized, the content of structural lipids was dropped once Symbiodiniaceae was expelled from the coral host. Overall, this work identified a set of metabolites as diagnostic markers of coral bleaching and provided insights into the biochemical and physiological mechanisms involved in coral bleaching.

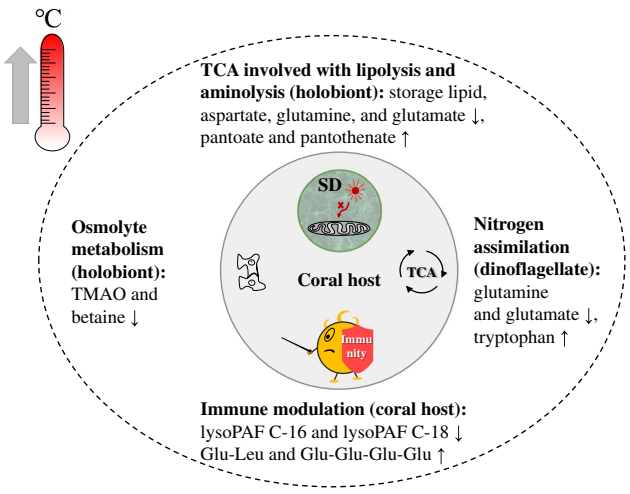

Fig. 6 The proposed biochemical adaption of the *P. decussata* coral holobiont exposed to thermal stress. SD represents symbiotic dinoflagellate

Supplementary Information The online version contains supplementary material available at https://doi.org/10.1007/s00216-022-04294-y.

Author contribution Conceived the project: J. Y. Pei, K. F. Yu. Obtained funding: K. F. Yu, J. Y. Pei. Mentorship: K. F. Yu. Field collections and indoor cultivation of corals: J. J. Zhang, W. F. Yu, J. J. Hu. Instrumental analysis: H. H. Chung. Bioinformatic analyses: J. Y. Pei, T. H. Kuo. Wrote the paper: J. Y. Pei, K. F. Yu, C. C. Hsu, T. H. Kuo.

Funding This work was supported by the National Natural Science Foundation of China (Nos. 42090041, 21665003, 42030502) and the Guangxi Natural Science Fund Project (Nos. 2018GXNSFAA281354, AD17129063, and AA17204074).

Declarations

Ethics approval All the animal protocols were approved by the Animal Care and Use Committee of Guangxi University (approval no. GXU–2022285).

Conflict of interest The authors declare no competing interests.

References

1. Ainsworth TD, Heron SF, Ortiz JC, Mumby PJ, Grech A, Ogawa D, Eakin CM, Leggat W. Climate change disables coral bleaching protection on the Great Barrier Reef. Science. 2016;352(6283):338–42.
2. Kwiatkowski L, Cox P, Halloran PR, Mumby PJ, Wiltshire AJ. Coral bleaching under unconventional scenarios of climate warming and ocean acidification. Nat Clim Change. 2015;5(8):777–81.
3. Hughes TP, Kerry JT, Simpson T. Large-scale bleaching of corals on the Great Barrier Reef. Ecology. 2018;99(2):501–601.
4. Hughes TP, Kerry JT, Alvarez-Noriega M, Alvarez-Romero JG, Anderson KD, Baird AH, Babcock RC, Beger M, Bellwood DR, Berkelmans R, Bridge TC, Butler IR, Byrne M, Cantin NE,

Comeau S, Connolly SR, Cumming GS, Dalton SJ, Diaz-Pulido G, Eakin CM, Figueira WF, Gilmour JP, Harrison HB, Heron SF, Hoey AS, Hobbs JPA, Hoogenboom MO, Kennedy EV, Kuo CY, Lough JM, Lowe RJ, Liu G, Cculloch MTM, Malcolm HA, Mcwilliam MJ, Pandolfi JM, Pears RJ, Pratchett MS, Schoepf V, Simpson T, Skirving WJ, Sommer B, Torda G, Wachenfeld DR, Willis BL, Wilson SK. Global warming and recurrent mass bleaching of corals. Nature. 2017;543(7645):373–7.

5. Hughes TP, Rodrigues MJ, Bellwood DR, Ceccarelli D, Hoegh-Guldberg O, McCook L, Moltschaniwskyj N, Pratchett MS, Steneck RS, Willis B. Phase shifts, herbivory, and the resilience of coral reefs to climate change. Curr Biol. 2007;17(4):360–5.
6. Cziesielski MJ, Liew YJ, Cui GX, Schmidt-Roach S, Campana S, Marondedze C, Aranda M. Multi-omics analysis of thermal stress response in a zooxanthellate cnidarian reveals the importance of associating with thermotolerant symbionts. Proc R Soc B Biol Sci. 1877;2018(285):20172654.
7. Parkinson JE, Baker AC, Baums IB, Davies SW, Grottoli AG, Kitchen SA, Matz MV, Miller MW, Shantz AA, Kenkel CD. Molecular tools for coral reef restoration: beyond biomarker discovery. Conserv Lett. 2020;13(1): e12687.
8. Lesser MP. Oxidative stress in marine environments: biochemistry and physiological ecology. Annu Rev Physiol. 2006;68:253–78.
9. Gruning NM, Lehrach H, Ralser M. Regulatory crosstalk of the metabolic network. Trends Biochem Sci. 2010;35(4):220–7.
10. Rivest EB, Chen CS, Fan TY, Li HH, Hofmann GE. Lipid consumption in coral larvae differs among sites: a consideration of environmental history in a global ocean change scenario. Proc R Soc B Biol Sci. 1853;2017(284):20162825.
11. Herrmann J, Abou Fayad A, Muller R. Natural products from myxobacteria: novel metabolites and bioactivities. Nat Prod Rep. 2017;34(2):135–60.
12. Roychoudhury A, Bieker A, Haussinger D, Oesterhelt F. Membrane protein stability depends on the concentration of compatible solutes - a single molecule force spectroscopic study. Biol Chem. 2013;394(11):1465–74.
13. Hill RW, Li C, Jones AD, Gunn JP, Frade PR. Abundant betaines in reef-building corals and ecological indicators of a photoprotective role. Coral Reefs. 2010;29(4):869–80.
14. Hillyer KE, Tumanov S, Villas-Boas S, Davy SK. Metabolite profiling of symbiont and host during thermal stress and bleaching in a model cnidarian-dinoflagellate symbiosis. J Exp Biol. 2016;219(4):516–27.
15. Quinn RA, Vermeij MJA, Hartmann AC, d'Auriac IG, Benler S, Haas A, Quistad SD, Lim YW, Little M, Sandin S, Smith JE, Dorrestein PC, Rohwer F. Metabolomics of reef benthic interactions reveals a bioactive lipid involved in coral defence. Proc R Soc B Biol Sci. 1829;2016(283):20160469.
16. Sogin EM, Putnam HM, Anderson PE, Gates RD. Metabolomic signatures of increases in temperature and ocean acidification from the reef-building coral. *Pocillopora damicornis* Metabolomics. 2016;12(4):1–12.
17. Hillyer KE, Dias DA, Lutz A, Wilkinson SP, Roessner U, Davy SK. Metabolite profiling of symbiont and host during thermal stress and bleaching in the coral Acropora aspera. Coral Reefs. 2017;36(1):105–18.
18. Roach TNF, Dilworth J, Martin CH, Jones AD, Quinn RA, Drury C. Metabolomic signatures of coral bleaching history. Nat Ecol Evol. 2021;5(4):495–503.
19. Williams A, Chiles EN, Conetta D, Pathmanathan JS, Cleves PA, Putnam HM, Su XY, Bhattacharya D. Metabolomic shifts associated with heat stress in coral holobionts. Sci Adv. 2021;7(1):eabd4210.
20. Farag MA, Meyer A, Ali SE, Salem MA, Giavalisco P, Westphal H, Wessjohann LA. Comparative metabolomics approach detects stress-specific responses during coral bleaching in soft corals. J Proteome Res. 2018;17(6):2060–71.
21. Boroujerdi AFB, Vizcaino MI, Meyers A, Pollock EC, Huynh SL, Schock TB, Morris PJ, Bearden DW. NMR-based microbial metabolomics and the temperature-dependent coral pathogen Vibrio coralliilyticus. Environ Sci Technol. 2009;43(20):7658–64.
22. Wang MX, Carver JJ, Phelan VV, Sanchez LM, Garg N, Peng Y, Nguyen DD, Watrous J, Kapono CA, Luzzatto-Knaan T, Porto C, Bouslimani A, Melnik AV, Meehan MJ, Liu WT, Criisemann M, Boudreau PD, Esquenazi E, Sandoval-Calderon M, Kersten RD, Pace LA, Quinn RA, Duncan KR, Hsu CC, Floros DJ, Gavilan RG, Kleigrewe K, Northen T, Dutton RJ, Parrot D, Carlson EE, Aigle B, Michelsen CF, Jelsbak L, Sohlenkamp C, Pevzner P, Edlund A, McLean J, Piel J, Murphy BT, Gerwick L, Liaw CC, Yang YL, Humpf HU, Maansson M, Keyzers RA, Sims AC, Johnson AR, Sidebottom AM, Sedio BE, Klitgaard A, Larson CB, Boya CA, Torres-Mendoza D, Gonzalez DJ, Silva DB, Marques LM, Demarque DP, Pociute E, O'Neill EC, Briand E, Helfrich EJN, Granatosky EA, Glukhov E, Ryffel F, Houson H, Mohimani H, Kharbush JJ, Zeng Y, Vorholt JA, Kurita KL, Charusanti P, McPhail KL, Nielsen KF, Vuong L, Elfeki M, Traxler MF, Engene N, Koyama N, Vining OB, Baric R, Silva RR, Mascuch SJ, Tomasi S, Jenkins S, Macherla V, Hoffman T, Agarwal V, Williams PG, Dai JQ, Neupane R, Gurr J, Rodriguez AMC, Lamsa A, Zhang C, Dorrestein K, Duggan BM, Almaliti J, Allard PM, Phapale P, Nothias LF, Alexandrovr T, Litaudon M, Wolfender JL, Kyle JE, Metz TO, Peryea T, Nguyen DT, VanLeer D, Shinn P, Jadhav A, Muller R, Waters KM, Shi WY, Liu XT, Zhang LX, Knight R, Jensen PR, Palsson BO, Pogliano K, Linington RG, Gutierrez M, Lopes NP, Gerwick WH, Moore BS, Dorrestein PC, Bandeira N. Sharing and community curation of mass spectrometry data with Global Natural Products Social Molecular Networking. Nat Biotechnol. 2016;34(8):828–37.
23. Hartmann AC, Petras D, Quinn RA, Protsyuk I, Archer FI, Ransome E, Williams GJ, Bailey BA, Vermeij MJA, Alexandrov T, Dorrestein PC, Rohwer FL. Meta-mass shift chemical profiling of metabolomes from coral reefs. Proc Natl Acad Sci USA. 2017;114(44):11685–90.
24. Ros M, Suggett DJ, Edmondson J, Haydon T, Hughes DJ, Kim M, Guagliardo P, Bougoure J, Pernice M, Raina JB, Camp EF. Symbiont shuffling across environmental gradients aligns with changes in carbon uptake and translocation in the reef-building coral Pocillopora acuta. Coral Reefs. 2021;40(2):595–607.
25. Yu XP, Yu KF, Liao ZH, Liang JY, Deng CQ, Huang W, Huang YH. Potential molecular traits underlying environmental tolerance of Pavona decussata and Acropora pruinosa in Weizhou Island, northern South China Sea. Mar Pollut Bull. 2020;156: 111199.
26. Yu WJ, Wang WH, Yu KF, Wang YH, Huang XY, Huang RY, Liao ZH, Xu SD, Chen XY. Rapid decline of a relatively high latitude coral assemblage at Weizhou Island, northern South China Sea. Biodivers Conserv. 2019;28(14):3925–49.
27. Qin ZJ, Yu KF, Wang YH, Xu LJ, Huang XY, Chen B, Li Y, Wang WH, Pan ZL. Spatial and intergeneric variation in physiological indicators of corals in the south china sea: insights into their current state and their adaptability to environmental stress. J Geophys Res-Oceans. 2019;124(5):3317–32.
28. Grottoli AG, Toonen RJ, van Woesik R, Thurber RV, Warner ME, McLachlan RH, Price JT, Bahr KD, Baums IB, Castillo KD, Coffroth MA, Cunning R, Dobson KL, Donahue MJ, Hench JL, Iglesias-Prieto R, Kemp DW, Kenkel CD, Kline DI, Kuffner IB, Matthews JL, Mayfield AB, Padilla-Gamino JL, Palumbi S, Voolstra CR, Weis VM, Wu HC. Increasing comparability among coral bleaching experiments. Ecol Appl. 2021;31(4): e0226.

29. Xia JG, Psychogios N, Young N, Wishart DS. MetaboAnalyst: a web server for metabolomic data analysis and interpretation. Nucleic Acids Res. 2009;37:W652–60.
30. Malul D, Holzman R, Shavit U. Coral tentacle elasticity promotes anout-of-phasemotion that improves mass transfer. Proc R Soc B Biol Sci. 1929;2020(287):20200180.
31. Sikorskaya TV, Ermolenko EV, Imbs AB. Effect of experimental thermal stress on lipidomes of the soft coral Sinularia sp. and its symbiotic dinoflagellates. J Exp Mar Biol Ecol. 2020;524:151295.
32. Kabeya N, Fonseca MM, Ferrier DEK, Navarro JC, Bay LK, Francis DS, Tocher DR, Castro LFC, Monroig O. Genes for de novo biosynthesis of omega-3 polyunsaturated fatty acids are widespread in animals. Sci Adv. 2018;4(5):eaar6849.
33. Imbs AB, Latyshev NA, Dautova TN, Latypov YY. Distribution of lipids and fatty acids in corals by their taxonomic position and presence of zooxanthellae. Mar Ecol Prog Ser. 2010;409:65–77.
34. Graham EM, Baird AH, Connolly SR, Sewell MA, Willis BL. Uncoupling temperature-dependent mortality from lipid depletion for scleractinian coral larvae. Coral Reefs. 2017;36(1):97–104.
35. Oku H, Yamashiro H, Onaga K. Lipid biosynthesis from [C-14]-glucose in the coral Montipora digitata. Fisheries Sci. 2003;69(3):625–31.
36. Yamashiro H, Oku H, Onaga K. Effect of bleaching on lipid content and composition of Okinawan corals. Fisheries Sci. 2005;71(2):448–53.
37. Davy SK, Allemand D, Weis VM. Cell biology of cnidarian-dinoflagellate symbiosis. Microbiol Mol Biol R. 2012;76(2):229–61.
38. Rosset S, Koster G, Brandsma J, Hunt AN, Postle AD, D'Angelo C. Lipidome analysis of Symbiodiniaceae reveals possible mechanisms of heat stress tolerance in reef coral symbionts. Coral Reefs. 2019;38(6):1241–53.
39. Berkelmans R, van Oppen MJH. The role of zooxanthellae in the thermal tolerance of corals: a 'nugget of hope' for coral reefs in an era of climate change. Proc R Soc B Biol Sci. 2006;273(1599):2305–12.
40. Nunez-Pons L, Bertocci I, Baghdasarian G. Symbiont dynamics during thermal acclimation using cnidarian-dinoflagellate model holobionts. Mar Environ Res. 2017;130:303–14.
41. d'Auriac IG, Quinn RA, Maughan H, Nothias LF, Little M, Kapono CA, Cobian A, Reyes BT, Green K, Quistad SD, Leray M, Smith JE, Dorrestein PC, Rohwer F, Deheyn DD, Hartmann AC. Before platelets: the production of platelet-activating factor during growth and stress in a basal marine organism. Proc R Soc B Biol Sci. 1884;2018(285):20181307.
42. van de Water JAJM, Ainsworth TD, Leggat W, Bourne DG, Willis BL, van Oppen MJH. The coral immune response facilitates protection against microbes during tissue regeneration. Mol Ecol. 2015;24(13):3390–404.
43. Gombos Z, Wada H, Hideg E, Murata N. The unsaturation of membrane lipids stabilizes photosynthesis against heat stress. Plant Physiol. 1994;104(2):563–7.
44. Quinn PJ, Joo F, Vigh L. The role of unsaturated lipids in membrane structure and stability. Prog Biophys Mol Biol. 1989;53(2):71–103.
45. Tchernov D, Gorbunov MY, de Vargas C, Yadav SN, Milligan AJ, Haggblom M, Falkowski PG. Membrane lipids of symbiotic algae are diagnostic of sensitivity to thermal bleaching in corals. Proc Natl Acad Sci USA. 2004;101(37):13531–5.
46. Sila A, Bougatef A. Antioxidant peptides from marine by-products: Isolation, identification and application in food systems. A review J Funct Foods. 2016;21:10–26.
47. Wang YG, Zhu FR, Han FS, Wang HA. Purification and characterization of antioxidative peptides from Salmon protamine hydrolysate. J Food Biochem. 2008;32(5):654–71.
48. Sato K, Egashira Y, Ono S, Mochizuki S, Shimmura Y, Suzuki Y, Nagata M, Hashimoto K, Kiyono T, Park EY, Nakamura Y, Itabashi M, Sakata Y, Furuta S, Sanada H. Identification of a hepatoprotective peptide in wheat gluten hydrolysate against d-galactosamine-induced acute hepatitis in rats. J Agr Food Chem. 2013;61(26):6304–10.
49. Wada S, Sato K, Ohta R, Wada E, Bou Y, Fujiwara M, Kiyono T, Park EY, Aoi W, Takagi T, Naito Y, Yoshikawa T. Ingestion of low dose pyroglutamyl leucine improves dextran sulfate sodium-induced colitis and intestinal microbiota in mice. J Agr Food Chem. 2013;61(37):8807–13.
50. Tanzi RE, Moir RD, Wagner SL. Clearance of Alzheimer's A beta peptide: the many roads to perdition. Neuron. 2004;43(5):605–8.
51. Lodwig EM, Hosie AHF, Bordes A, Findlay K, Allaway D, Karunakaran R, Downie JA, Poole PS. Amino-acid cycling drives nitrogen fixation in the legume - Rhizobium symbiosis. Nature. 2003;422(6933):722–6.
52. Pernice M, Meibom A, Van Den Heuvel A, Kopp C, Domart-Coulon I, Hoegh-Guldberg O, Dove S. A single-cell view of ammonium assimilation in coral-dinoflagellate symbiosis. Isme J. 2012;6(7):1314–24.
53. Nandi PK, Bera A, Sizaret PY. Osmolyte trimethylamine N-oxide converts recombinant alpha-helical prion protein to its soluble beta-structured form at high temperature. J Mol Biol. 2006;362(4):810–20.
54. Raymond JA, DeVries AL. Elevated concentrations and synthetic pathways of trimethylamine oxide and urea in some teleost fishes of McMurdo Sound. Antarctica Fish Physiol Biochem. 1998;18(4):387–98.
55. Wu WK, Chen CC, Liu PY, Panyod S, Liao BY, Chen PC, Kao HL, Kuo HC, Kuo CH, Chiu THT, Chen RA, Chuang HL, Huang YT, Zou HB, Hsu CC, Chang TY, Lin CL, Ho CT, Yu HT, Sheen LY, Wu MS. Identification of TMAO-producer phenotype and host-diet-gut dysbiosis by carnitine challenge test in human and germ-free mice. Gut. 2019;68(8):1439–49.
56. Bourne D, Iida Y, Uthicke S, Smith-Keune C. Changes in coral-associated microbial communities during a bleaching event. Isme J. 2008;2(4):350–63.